Thermal properties of alkyloctamethylferrocenium salts with TFSA and TCNE (TFSA = bis(trifluoromethylsulfonyl)amide and TCNE = tetracyanoethylene)

Funasako, Yusuke

Abe, kenichi

Mochida, Tomoyuki

(Citation)
Thermochimica Acta,532:78-82

(Issue Date)
2012-05-20

(Resource Type)
journal article

(Version)
Accepted Manuscript

(URL)
https://hdl.handle.net/20.500.14094/90001810

Thermal properties of alkyloctamethylferrocenium salts with TFSA and TCNE (TFSA = bis(trifluoromethylsulfonyl)amide; TCNE = tetracyanoethylene)

Yusuke Funasako, Ken-ichi Abe, and Tomoyuki Mochida*

Department of Chemistry, Graduate School of Science, Kobe University, Rokkodai, Nada, Hyogo 657-8501, Japan

Abstract

Butyl- and hexyloctamethylferrocenium salts with bis(trifluoromethylsulfonyl)amide (TFSA) and tetracyanoethylene (TCNE) were prepared, and their thermal properties were investigated by differential scanning calorimetry (DSC) measurements. The TFSA salts were ionic liquids with melting points of 34.4 °C and 27.7 °C, respectively. The TCNE salts were prepared by annealing the mixture of alkyloctamethylferrocene and TCNE. These salts exhibited high melting points of 100.2 °C and 80.9 °C, respectively; they were thermally unstable at higher temperatures. A butyloctamethylferrocenium salt with PCNP (pentacyanopropenide), obtained by a reaction with TCNE under ambient conditions, was crystallographically characterized. The structure was severely disordered, consisting of alternately stacked cations and anions.

Keywords: Ionic liquids, Alkyloctamethylferrocene, Bis(trifluoromethylsulfonyl)amide, Tetracyanoethylene, Thermal properties

---

*Corresponding Author. Tel./fax: +81-78-803-5679

E-mail address: tmochida@platinum.kobe-u.ac.jp (T. Mochida)

1. Introduction

Ionic liquids (ILs) are interesting materials from the viewpoint of fundamental physical chemistry and electrochemistry [1]. Most ILs involve onium cations such as imidazolium, ammonium, and phosphonium cations. Bis(trifluoromethylsulfonyl)amide (TFSA) and its derivatives are frequently used as their counteranions [2]. Recently, metal-containing ILs with additional functionalities have been prepared [3]. We have developed various ferrocene-based ILs composed of alkylferrocenium [4a] and ferrocenylimidazolium cations [4b,c].

In this study, salts of butyloctamethylferrocene (**1**) and hexyloctamethylferrocene (**2**) with TFSA and tetracyanoethylene (TCNE) (Fig. 1) were prepared, and their thermal properties were investigated. The magnetic properties of **1·TFSA** are reported elsewhere [5]. The use of octamethylferrocenium cations lends greater air stability to the ILs. Thus far, ILs with cyano-containing anions such as $[N(CN)_2]^-$, $[C(CN)_3]^-$, $[C(CN)_2X]^-$ (X = SO_2CF_3, NO, NO_2), and PCNP (pentacyanopropenide; Fig. 1b) have been reported [6], but there seems to be no ILs containing TCNE. The TCNE anion is a radical; its complexes exhibit interesting magnetic properties. For example, decamethylferrocene–TCNE is the first molecular ferromagnet (T_c = 4.8 K) [7]. In addition, TCNE can form complexes that do not adhere to 1:1 donor/acceptor stoichiometry [8]. In this study, we found that mixing TCNE and alkyloctamethylferrocenes and subsequent annealing afforded the desired TCNE salts.

The TCNE anion reacts with oxygen to form the PCNP anion [7,9]. We herein describe the crystal structure of **1·PCNP**, which was obtained in the reaction using TCNE.

2. Results and discussion

2.1. Preparation and thermal properties

Differential scanning calorimetry (DSC) measurements of **1** and **2** revealed that they show only glass transitions, at T_g of –87.9 °C and –82.7 °C, respectively, on cooling from the liquid state.

During heating, however, crystallization occurred at around –12.5 °C and –33.8 °C, respectively. Their melting points (T_m) were 27.6 °C and 22.1 °C, respectively. A phase transition with a small entropy change was observed in both **1** and **2**, appearing as a shoulder at approximately 5 K below T_m. The values of T_m/T_g for **1** and **2** are 0.63 and 0.65, respectively, which are consistent with the empirical relationship $T_g/T_m \approx 2/3$ [10].

1·TFSA and **2·TFSA** were prepared by reactions of alkyloctamethylferrocene and AgTFSA [5]. **1·TCNE** and **2·TCNE** were obtained by annealing the mixture of alkyloctamethylferrocene and TCNE in a DSC pan, or by simply grinding the mixture with an agate and mortar under a nitrogen atmosphere. For technical reasons, samples with a donor–acceptor molar ratio of 0.51:0.49 were used for measurements. In the infrared spectrum of **1·TCNE**, C≡N stretching peaks [11] were observed at 2184 cm^{-1} and 2145 cm^{-1}, which indicated the formation of a 1:1 salt containing the TCNE anion and ferrocenium cation. The TCNE salts were unstable in air.

Table 1 lists the melting points (T_m) and melting entropies (ΔS_m) of **1**, **2**, and their salts with TFSA and TCNE, as determined by the DSC measurements. The values of ΔS_m for **1**, **2**, and **2·TFSA** are the sums of their transition entropies from the stable phase to the liquid state. Compared to the melting points of **1** and **2**, the melting points of the TFSA salts (34.4 °C for **1·TFSA** and 27.7 °C for **2·TFSA**) were higher by approximately 6 K, while those of the TCNE salts (100.2 °C for **1·TCNE** and 80.9 °C for **2·TCNE**) were much higher. The high melting points of the latter salts are probably due to the planarity and high symmetry of the anion, leading to stronger intermolecular forces.

In the case of both TFSA and TCNE salts, increasing the alkyl chain length from $n = 4$ (salts of **1**) to $n = 6$ (salts of **2**) led to a decrease in melting point, which is in accordance with the general tendency observed in conventional ILs [1e]. One methylene group represents an entropy of 10.6 J K^{-1} mol^{-1} in molecular compounds with long alkyl chains [12]. The values of ΔS_m, however, for the TFSA salts and their precursors were comparable (81–86 J K^{-1} mol^{-1}), while the value for the TCNE salts increased by 16.1 J K^{-1} mol^{-1} on increasing the alkyl chain length from $n = 4$ to $n = 6$. Hence

the effect of the increase in the alkyl chain length is small; their thermal properties are probably dominated by the octamethylferrocenyl moiety, which has much larger volume than the alkyl chains.

2.2. Thermal properties of TFSA salts

1·TFSA underwent only melting (T_m = 34.4 °C) and crystallization (T_c = 18.9 °C), exhibiting no crystalline phase transitions. By contrast, **2·TFSA** exhibited three crystalline phases (phases I–III), and phase I melting at 26.3 °C. Figure 2 shows the Gibbs free energy diagrams for **2·TFSA**, in which the temperature dependence is approximated by straight lines. Upon cooling from the liquid state, crystallization to phase I occurred, followed by a transition to a metastable phase (phase II). During the heating run, a reverse phase sequence was often traced, but the transformation to phase III occurred occasionally.

DSC traces of **2·TFSA** are shown in Fig. 3. Upon cooling at 10 K min^{-1} from the liquid state, crystallization to phase I occurred at –10.6 °C, which was immediately followed by a transition to phase II (Fig. 3a). Upon cooling at 1 K min^{-1}, these peaks could be separated, and upon heating at 1 K min^{-1} from phase II, a reverse phase sequence was observed. However, as noted above, heating phase II at 10 K min^{-1} occasionally gave rise to an exothermic transition to phase III, as can be seen in Fig. 3a (heating run). In this figure, the transition occurred at –10 °C, which was followed by a transition to phase I at 21.4 °C and melting at 27 °C. A DSC pattern as shown in Fig. 3b was also observed several times, which revealed phase transitions from phase II to phase I at –2.1 °C (ΔH = 9.4 kJ mol^{-1}, ΔS = 34.5 J mol^{-1} K^{-1}), from phase I to phase III with a broad exothermic peak at 10 °C, and again back to phase I, and subsequent melting. This re-entrant behavior was often observed when the compound was heated directly after crystallization. Cooling from phase I at 2 K min^{-1} gave phase III, as shown in Fig. 3c. Phase I is probably a highly disordered phase, in view of the small value of ΔS (21 J mol^{-1} K^{-1}) associated with its melting.

2.3. Thermal properties of TCNE salts

The dependence of the thermal behavior of alkyloctamethylferrocenium–TCNE salts on the mixing ratio of alkyloctamethylferrocene and TCNE was investigated for various mixing ratios, $(\mathbf{1})_{1-x}(\mathrm{TCNE})_x$. DSC traces for an equimolar mixture (x = 0.49) before and after annealing are shown in Fig. 4. In the first heating run before annealing, glass transition (T_g = –88.1 °C), crystallization (T_c = –38.6 °C), and melting (T_m = 27.4 °C) corresponding to those of **1** contained in the mixture were observed (Fig. 4, cycle 1). Upon further heating, an exothermic peak corresponding to the formation of **1·TCNE** was observed at around 85 °C, at which the sample was annealed for 3 min and then cooled. The enthalpy of the formation of the salt estimated from the exothermic peak was approximately 38 kJ mol^{-1}. In the second heating run (Fig. 4, cycle 2), the peaks of the precursor disappeared, and a melting peak was observed for the salt (T_m = 100.2 °C). Upon repetition of the cycle, the melting point decreased by approximately 3 K, which can be attributed to slight decomposition of the salt. A similar result was obtained for **2·TCNE**. However, characterization of this salt was more difficult owing to the gradual formation of the salt upon heating, which was accompanied by partial melting and decomposition.

DSC traces of $(\mathbf{1})_{1-x}(\mathrm{TCNE})_x$ for various values of x (x < 0.5) after annealing are shown in Fig. 5. As the proportion of TCNE was increased, the peaks corresponding to crystallization and melting of excess **1** decreased, disappearing at $x \approx 0.5$. This result indicated the formation of a 1:1 salt. The possible formation of a 1:2 salt in the TCNE-rich region (x > 0.5) could not be examined because a rapid exothermic decomposition reaction occurred after melting in this region. Since the melting point of TCNE (T_m = 199 °C, ΔH_m = 24.9 kJ mol^{-1} [13]) is higher than that of the 1:1 salt, the melting of excess TCNE could not be observed owing to decomposition. The melting points of the 1:1 salt and residual alkyloctamethylferrocene for $(\mathbf{1})_{1-x}(\mathrm{TCNE})_x$ are listed in Table 2. The melting temperatures of the 1:1 salt and alkyloctamethylferrocene were found to be almost independent of x. Although the slight scattering of the values of T_m is probably due to an effect of decomposition, the

tendency of T_m to decrease below x = 0.19 seems to indicate the onset of a steep decrease in the vicinity of x = 0, where a eutectic point probably exists. The melting peaks became slightly broader as the ratio approached 1:1.

In this study, the use of TCNE allowed convenient preparation of salts by mixing and annealing, but their melting points were high, and decomposition in the TCNE-rich region precluded the determination of the complete phase diagram. In the case of an IL formed by an acid–base reaction of imidazole and HTFSA (T_m = 73 °C), a phase diagram with respect to the mixing ratio has been reported, revealing a clear eutectic behavior [14]. Phase diagrams of charge-transfer (CT) complexes of alkylbenzenes and TCNE, which form neutral complexes with ratios of 1:1 and 2:1, have been reported [13].

2.4. Crystal structure of butyloctamethylferrocenium–PCNP

Dark green crystals of **1·PCNP** were obtained by slow diffusion of **1** and TCNE in diethyl ether. The presence of infrared C≡N stretching peaks at 2200 cm^{-1} [15] indicated that PCNP was the only anion in the isolated crystals. The anion was formed probably because of contamination by oxygen during manipulation. Under strict exclusion of oxygen, only powdered CT salts were obtained, which suggests that **1·TCNE** has poor crystallinity.

The packing diagram of **1·PCNP**, projected along the *c*-axis, is shown in Fig. 6. In the crystal, the cations and anions are stacked alternately along the *b*-axis via π–π contacts. The C_5Me_4H ring and an adjacent PCNP are well overlapped, but the C_5Me_4Bu ring and an adjacent PCNP are in a slipped configuration due to steric hindrance of the butyl group. In the cation, the average Fe–C(Cp) distance is 2.085 Å, which is comparable to the value observed for the decamethylferrocenium cation [16]. It should be noted that the structure was severely disordered. The four methyl groups in the C_5Me_4H ring were observed to be disordered over five sites with an occupancy of 0.8. In addition, the C_5Me_4Bu ring, together with the butyl group, exhibited a two fold disorder. The PCNP anion

exhibited a two-fold disorder, with two inverted PCNP molecules overlapping and sharing one C–C bond, as shown schematically in Fig. 7. These extensive disorders, which are probably responsible for the high *R* value (12.4%), are consistent with the nearly symmetrical crystal environment around the cation and anion. The crystal structures of [decamethylferrocenium][PCNP] [7] and the PCNP salts of triaminoguanidine derivatives [17] are comparable examples; the latter involves a disordered anion.

3. Conclusion

Alkyloctamethylferrocenium salts [*R* = butyl (**1**) and hexyl (**2**)] with TFSA were found to be room-temperature ILs; their melting points were slightly higher than those of their precursors (**1** or **2**). Alkyloctamethylferrocenium salts with TCNE anions were conveniently prepared by annealing the mixture of alkyloctamethylferrocene and TCNE. Their melting points, however, were much higher than those of the TFSA salts, probably owing to the planarity and high symmetry of the anion. The donor–acceptor ratio of the TCNE salts was 1:1, which was independent of the mixing ratio, and these salts were thermally unstable above their melting points. Single crystals of TCNE salts could not be isolated, and a PCNP salt of **1** was obtained instead, probably because of contamination by oxygen. This salt exhibited alternate stacking of the cations and anions.

4. Experimental

4.1. General methods

The preparation of **1**, **2**, and their TFSA salts was performed as reported elsewhere [5]. Sample purities (> 99.7%) were checked by elemental analyses. TCNE was purchased from TCI Co. Ltd. and used after recrystallization from chlorobenzene. All manipulation of TCNE salts was carried out in a glove box under a nitrogen atmosphere. Solvents were degassed by bubbling with nitrogen before use. Infrared spectra were recorded using KBr pellets on a JASCO FT-IR 230 spectrometer.

DSC measurements were performed using a Q100 differential scanning calorimeter (TA instruments) at 10 K min^{-1}, and other rates when necessary, in a temperature range down to 100 K. For the DSC measurements of $(\mathbf{1})_{1-x}(TCNE)_x$ and $(\mathbf{2})_{1-x}(TCNE)_x$, samples with a total mass of about 5 mg were placed in Al hermetic pans under a nitrogen atmosphere and subjected to measurement. The slight deviation from the 1:1 donor-acceptor ratio (0.51:0.49) for **1·TCNE** and **2·TCNE** occurred owing to the difficulty in loading the starting materials into the DSC pans.

4.2. X-ray crystallography

Dark green single crystals of **1·PCNP** for X-ray structure determination were obtained by slow diffusion of butyloctamethylferrocene and TCNE in an H-shaped pyrex cell, using diethyl ether as a solvent. X-ray diffraction data were collected at 100 K on a Bruker SMART APEX CCD diffractometer equipped with a graphite crystal incident beam monochromator using MoKα radiation (λ = 0.71073 Å). The data were corrected for absorption using the SADABS program [18]. The structures were solved by the direct method (SHELXS 97 [19]) and expanded using Fourier techniques. Crystallographic parameters are listed in Table 3. The ORTEP-3 [20] program was used for drawing the packing diagram. Crystallographic data for the structure in this paper have been deposited with the Cambridge Crystallographic Data Centre as supplementary publication no. CCDC 778957. These data can be obtained free of charge from the Cambridge Crystallographic Data Centre at www.ccdc.cam.ac.uk/data_request/cif.

Acknowledgements

We thank T. Inagaki and Y. Furuie for their help with sample preparation and DSC measurements. This work was supported by a Grant-in-Aid for Scientific Research (No. 21350077) from Japan Society for the Promotion of Science (JSPS). M. Nakama (WarpStream Ltd., Tokyo) is acknowledged for providing Web-DB systems.

References

[1] (a) R. D. Rogers, K. R. Seddon (Eds.), Ionic Liquids: Industrial Applications to Green Chemistry, ACS Symposium Series, American Chemical Society, Washington DC, 2002. (b) A. Stark, K. R. Seddon, in Kirk-Othmer Encyclopedia of Chemical Technology, 5th ed., ed. by Kirk-Othmer, Wiley-Interscience, 2007, Vol. 26, pp. 836. (c) M. Armand, F. Endres, D. R. MacFarlane, H. Ohno, B. Scrosati, Nature Mater. 8 (2009) 621–629. (d) P. Hapiot, C. Lagrost, Chem. Rev. 108 (2008) 2238–2264. (e) N. V. Plechkova, K. R. Seddon, Chem. Soc. Rev. 37 (2008) 123–150.

[2] (a) H.Weingärtner, Angew. Chem., Int. Ed. 47 (2008) 654. (b) S. Lee, Chem. Commun. (2006) 1049. (c) Y. Yoshida, G. Saito, Phys. Chem. Chem. Phys. 12 (2010) 1675–1684.

[3] (a) W. Wang, R. Balasubramanian, R. W. Murray, J. Phys. Chem. C, 112 (2008) 18207–18216. (b) Y. Gao, B. Twamley, J. M. Shreeve, Inorg. Chem. 43 (2004) 3406–3412. (c) H. Matsumoto, JP. Patent 277393, 2003. (d) C. K. Lee, K.-M. Hsu, C.-H. Tsai, C. K. Lai, I. J. B. Lin, Dalton Trans. (2004) 1120–1126. (e) M. Iida, C. Baba, M. Inoue, H. Yoshida, E. Taguchi, H. Furusho, Chem. Eur. J. 14 (2008) 5047–5056.

[4] (a) T. Inagaki, T. Mochida, Chem. Lett. 39 (2010) 572–573. (b) Y. Miura, F. Shimizu, T. Mochida, Inorg. Chem. 49 (2010) 10032–10040 (2010). (c) T. Mochida, Y. Miura, F. Shimizu, Cryst.Growth Des. (2011), in press.

[5] Y. Funasako, T. Mochida, T. Inagaki, T. Sakurai, H. Ohta, K. Furukawa, T. Nakamura, submitted.

[6] (a) Y.Yoshida, K. Muroi, A. Otsuka, G. Saito, M. Takahashi, T.Yoko, Inorg. Chem. 43 (2004) 1458–1462. (b) Y. Yoshida, M. Kondo, G. Saito, J. Phys. Chem. B 113 (2009) 8960–8966.

[7] J. S. Miller, J. C. Calabrese, H. Rommelmann, S. Chittipeddi, J. H. Zhang, W. M. Reiff, A. J. Epstein, J. Am. Chem. Soc. 109 (1987) 769–781.

[8] A.Quazi, W. M. Reiff, R. U. Kirss, Hyperfine Int. 93 (1994) 1597–1603.

[9] M. Rosenblum, R. W. Fish, C. Bennett, J. Am. Chem. Soc. 86 (1964) 5166–5170.

[10] D. Turnbull, M.H. Cohen, in Modern Aspect of the Vitreous State, J.D. Mackenzie (Ed.) Butterworth, London, 1 (1960) 38.

[11] J. S. Miller, D. T. Glatzhofer, D. M. O'Hare, W. M. Reiff, A. Chakraborty, A. J. Epstein, Inorg. Chem. 28 (1989) 2930–2939.

[12] (a) M. Sorai, K. Tsuji, H. Suga, S. Seki, Mol. Cryst. Liq. Cryst., 59 (1980) 33–58. (b) Y. Shimizu, Y. Ohte, Y. Yamamura, K. Saito, Chem. Phys. Lett. 470 (2009) 295–299.

[13] M. Radomska, R. Radomski, J. Therm. Anal. 37 (1991) 693–704.

[14] A. Noda, Md. A. B. H. Susan, K. Kudo, S. Mitsushima, K. Hayamizu, M. Watanabe, J. Phys. Chem. B 107 (2003) 4024–4033.

[15] K. W. Hipps, U. Geiser, U. Mazur, R. D. Willett, J. Phys. Chem. 88 (1984) 2498–2504.

[16] A. S. Perucha, M. Bolte, Acta Cryst. E63 (2007) m1703.

[17] H. Gao, Z. Zeng, B. Twamley, J. M. Shreeve, Chem. Eur. J. 14 (2008) 1282–1290.

[18] G. M. Sheldrick, SADABS. Program for Semi-empirical Absorption Correction, University of Göttingen, Germany, 1996.

[19] G. M. Sheldrick, Program for the Solution for Crystal Structures; University of Göttingen, Germany, 1997.

[20] ORTEP-3 for Windows. L.J. Farrugia, J. Appl. Cryst. 30 (1997) 565.

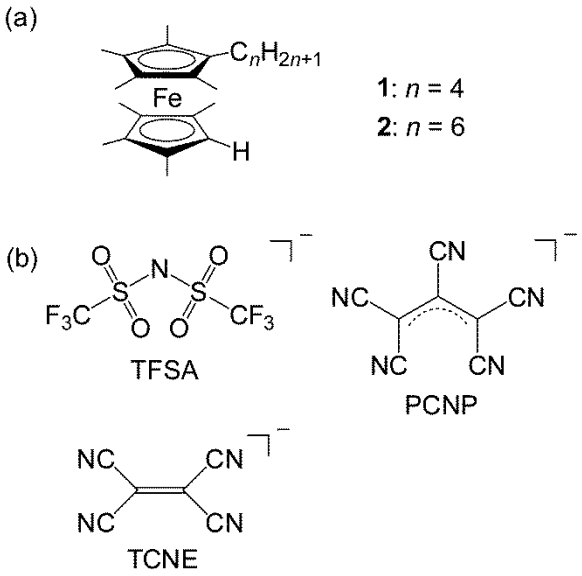

Fig. 1. Chemical formulas of (a) alkyloctamethylferrocenes and (b) anions used in this study.

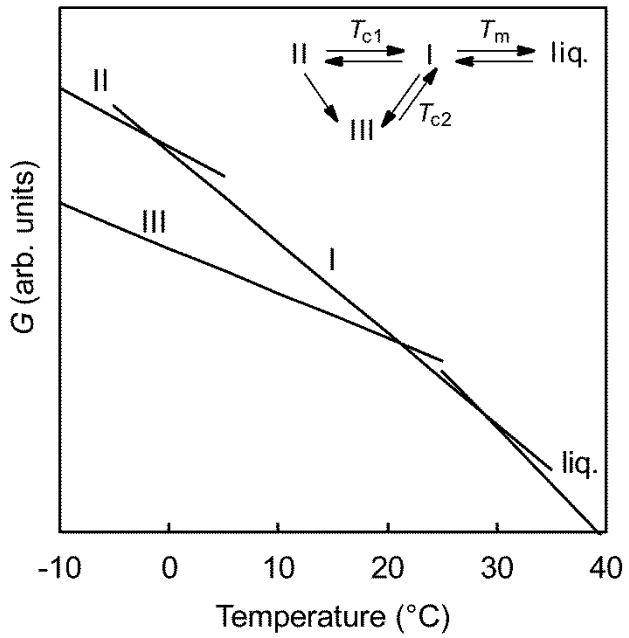

Fig. 2. Gibbs free energy curves of **2·TFSA**. The inset shows a schematic illustration of the phase diagram.

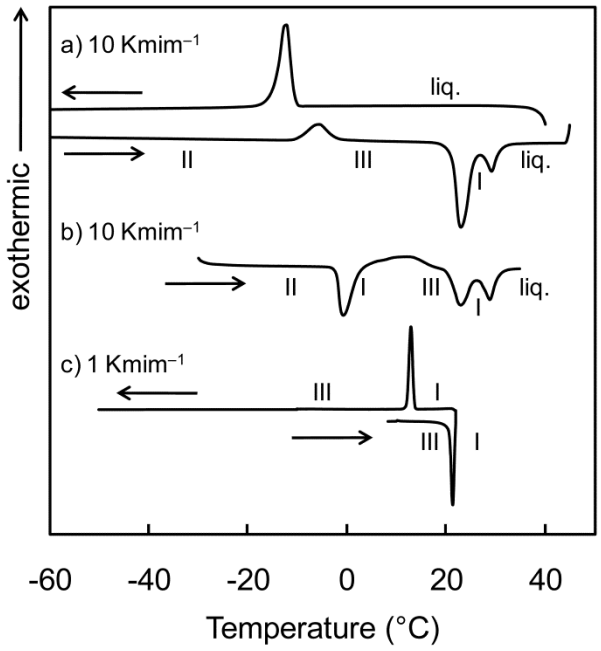

Fig. 3. DSC traces of **2·TFSA** (see text).

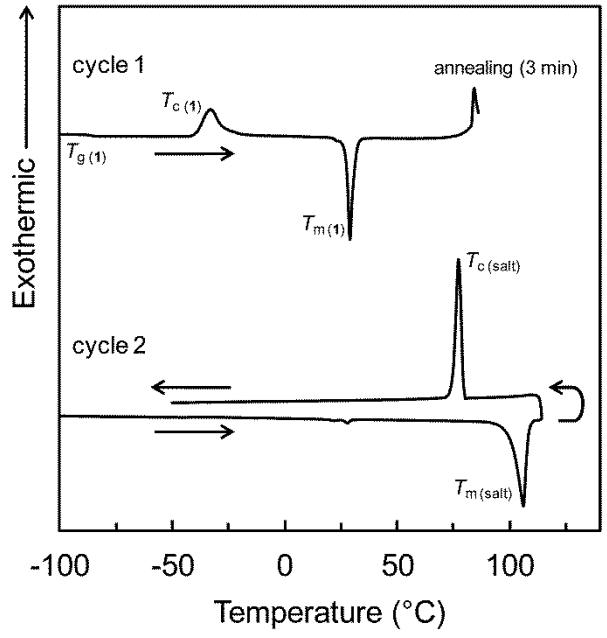

Fig. 4. DSC traces of an equimolar mixture of **1** and TCNE (x = 0.49) before (cycle 1) and after (cycle 2) annealing. $T_{g\,(1)}$, $T_{c\,(1)}$, and $T_{m\,(1)}$ are the glass transition, crystallization, and melting temperatures of **1**, respectively. $T_{m\,(salt)}$ and $T_{c\,(salt)}$ are the melting and crystallization temperatures, respectively, of **1·TCNE**.

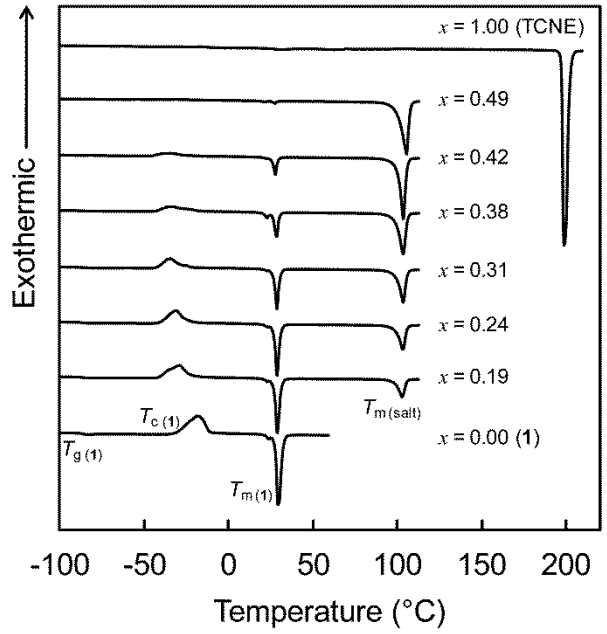

Fig. 5. DSC traces of $(\mathbf{1})_{1-x}(\mathrm{TCNE})_x$ for various x ($x < 0.5$). $T_{g\ (1)}$, $T_{c\ (1)}$, and $T_{m\ (1)}$ are the glass transition, crystallization, and melting temperatures of **1**, respectively. $T_{m\ (salt)}$ denotes the melting temperature of **1·TCNE**.

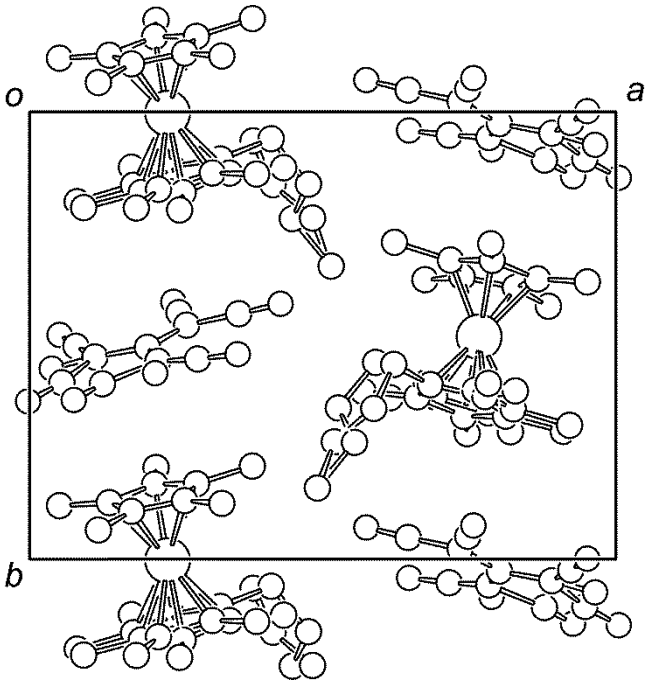

Fig. 6. Packing diagram of **1·PCNP** viewed along the *c*-axis.

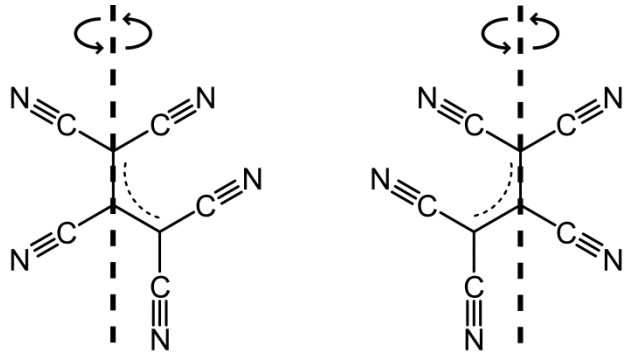

Fig. 7. Schematic illustration of two-fold disorder of the PCNP anion with a 0.5 occupancy in **1·PCNP**.

Table 1 Melting points (T_m) and melting entropies[a)] (ΔS_m) of **1**, **2**, and their TFSA and TCNE salts.

	T_m (°C)	ΔS_m (J K^{-1} mol^{-1})
1	27.6	80.6
2	22.1	84.7
1·TFSA	34.4	86.3
2·TFSA	27.7	84.6
1·TCNE[a)]	100.2	93.9
2·TCNE[a,b)]	80.9	110.0

[a)]Sum of transition entropies. [b)]Determined for as-prepared samples in a DSC pan with a mixing ratio of 0.51:0.49.

[c)]Melting accompanied by slight decomposition.

Table 2 Thermal properties[a)] of $(\mathbf{1})_{1-x}(TCNE)_x$ obtained by DSC measurement.

x	$T_{m\ (salt)}$ (°C)	$T_{c\ (\mathbf{1})}$ (°C)	$T_{g\ (\mathbf{1})}$ (°C)	$T_{m\ (\mathbf{1})}$ (°C)
0.00	—	–29.1	–89.0	27.6
0.06	92.3	–39.0	–87.9	27.5
0.19	98.9	–40.6	–88.2	27.3
0.24	100.6	–40.1	–88.2	27.2
0.31	100.2	–41.6	–88.3	27.1
0.34	98.7	–42.4	–89.5	27.1
0.38	100.0	–42.4	–87.2	26.9
0.42	100.9	–44.8	–89.4	26.2
0.46	100.4	–43.6	–90.0	25.6
0.49	100.2	—	—	—

[a)]Onset temperatures of endothermic peak ($T_{m\ (salt)}$ and $T_{m\ (\mathbf{1})}$), heat capacity change ($T_{g(\mathbf{1})}$), and exothermic peak ($T_{c\ (\mathbf{1})}$).

Table 3 Crystallographic parameters for **1·PCNP**.

Formula	C30 H33 Fe N5
Formula weight	519.46
T / K	100
Crystal system	Monoclinic
Space group	$P\,2_1/c$
a / Å	15.906(3)
b / Å	11.296(2)
c / Å	16.392(3)
β / deg	111.770(2)
V / Å^3	2735.2(9)
Z	4
D_{calc} / g cm^{-3}	1.261
μ / mm^{-1}	0.572
Reflections collected	15177
Independent reflections	6184 (R_{int} = 3.2%)
$F(000)$	1096
Parameters	474
Final R_1, wR_2 ($I > 2\sigma$)	R_1 = 0.1240, wR_2 = 0.2522
Final R_1, wR_2 (all data)	R_1 = 0.1483, wR_2 = 0.2638
Goodness of fit on F^2	1.155